IASMiRT

SMiRT 26
50 Anniversary Berlin/Potsdam

Transactions, SMiRT-26
Berlin/Potsdam, Germany, July 10-15, 2022
Division V

Study on influence evaluation of internal equipment installed in structure subjected to projectile impact

Yukihiko Okuda[1], Zuoyi Kang[2], Akemi Nishida[3], Haruji Tsubota[4] and Yinsheng Li[5]

[1] Assistant Principal Researcher, Japan Atomic Energy Agency, Ibaraki, JAPAN
(okuda.yukihiko@jaea.go.jp)
[2] Research Engineer, Japan Atomic Energy Agency, Ibaraki, JAPAN
[3] Deputy Division Head, Japan Atomic Energy Agency, Ibaraki, JAPAN
[4] Researcher, Japan Atomic Energy Agency, Ibaraki, JAPAN
[5] Division Head, Japan Atomic Energy Agency, Ibaraki, JAPAN

ABSTRACT

When a projectile collides with a nuclear building, stress waves are generated at the impacted area and propagate to the interior of the building through the building structure. Assessing the influence of dynamic responses generated by the projectile impact on the internal equipment is crucial because stress waves can excite high-frequency vibrations of the internal equipment , influencing their functionality. Therefore, we performed a projectile impact test on a reinforced concrete (RC) structure that models a nuclear building with internal equipment. This paper presents the test method, the measuring method, and the investigation results of the impact response characteristics of the RC structure subjected to projectile impact.

INTRODUCTION

After the 2011 Fukushima Daiichi Nuclear Power Plant (NPP) accident, new regulatory requirements stipulated by the Nuclear Regulation Authority of Japan were introduced in 2013 for the safety evaluation of nuclear facilities subjected to projectile impacts induced by tornadoes or aircraft. It is crucial to develop a numerical analysis method and confirm its validity via test data to evaluate the influence on NPP buildings and internal equipment due to projectile impact.

Overall, many empirical formulas for evaluating local damage to reinforced concrete (RC) structures have been proposed. Most formulas were derived based on impact tests using rigid projectiles colliding with RC structures at a normal impact. Kennedy (1976). and Li et al. (2005) reviewed and summarized these empirical formulas. Stress waves induced in a RC structure by an impact force can propagate inside the structure, which must be considered in the design or evaluation of the structure and its components installed within.

In 2016, the Organization for Economic Cooperation and Development/Nuclear Energy Agency(OECD/NEA) launched a new impact analysis benchmark project, Improving Robustness Assessment Methodologies for Structures Impacted by Missiles (IRIS Phase 3). IRIS3 extends the knowledge gained from previous IRIS2010 and IRIS2012 projects and focuses on the behavior of walls impacted by missiles and the stress waves propagating throughout the structure. The IRIS3 final workshop was held in Feb. 2022, and calibration analysis results conducted by many organizations were presented and discussed. The results showed that the modeling methods of the specimen's support had a significant effect on the vibration behavior.

This research obtains data on stress wave propagation in a building and the impact response of the equipment contained in the building, and develops an impact response analysis method that considers the coupling of the building and equipment. Projectile impact tests were conducted using a projectile simulating

an aircraft, and a beam-like structure simulating equipment with a part (pseudo equipment and a pseudo part) was installed on the inner wall of the RC structure simulating the building. Test data were obtained for evaluating the stress wave propagation in the building and the impact response on the RC structure, the pseudo equipment, and the pseudo part after the projectiles impact. Specifically, the projectile impact tests were conducted by vertically impacting the projectile simulating an aircraft on the RC structural specimen's outer wall, and after three impact tests, the impact test was completed due to cracking on the impacted surface's backside. This paper provides the detailed conditions of the impact tests, the test specimens used in these impact tests, the test methods, and test results. Also, an overview of the static compression test of the projectile and impact force measurement tests are shown.

TEST METHOD

We conducted impact tests using an RC structure simulating the outer walls of a nuclear facility building, internal equipment inside the building, and parts in the equipment. Then, we obtained test data related to impact response and stress wave propagation in the building after the projectile's impact. This section presents the test method.

Test equipment

Impact tests were conducted using a high-pressure pneumatic launcher (Fig. 1). The RC structure as a target is installed inside the ballistic protection shelter and a projectile is ejected through the cannon tube. The constraint conditions for impact tests with the RC structure were hoisted in all cases to simplify the effect of constraints in this study. The RC structure's four corners were fixed with bolts in a room and hoisted by rods through a jig.

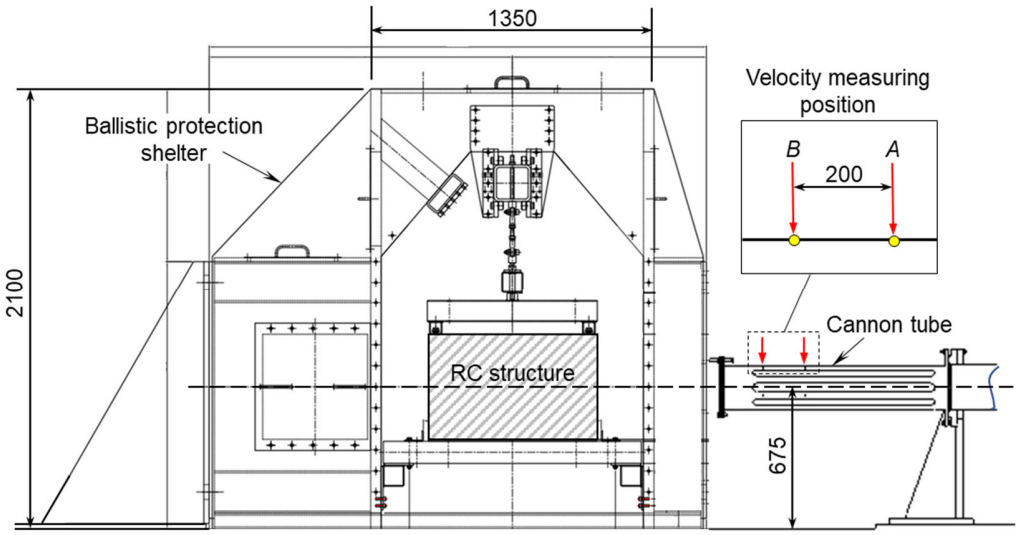

Figure 1. Experimental setup (unit: mm).

RC Structure and pseudo equipment

Figure 2 shows the outline of the projectile impact test. The dimensions of the RC structure were 500 mm (length) × 800 mm (width) × 500 mm (height), and the plate thickness was 80 mm on all sides. The RC structure has four sides surrounded by RC slabs, and two sides are open. Table 1 summarizes the RC structure's specifications. The average compressive strength of concrete was greater than 40 N/mm^2. The

table describes the rebar diameter, layers, and reinforcement ratio, and the maximum aggregate size was 10 mm. Pseudo equipment was attached to the RC structure (Fig. 2). The pseudo equipment is a beam-like structure, designed to have a primary natural frequency of approximately 35 Hz. The pseudo part is designed for approximately 200 Hz and attached to the tip of the pseudo equipment.

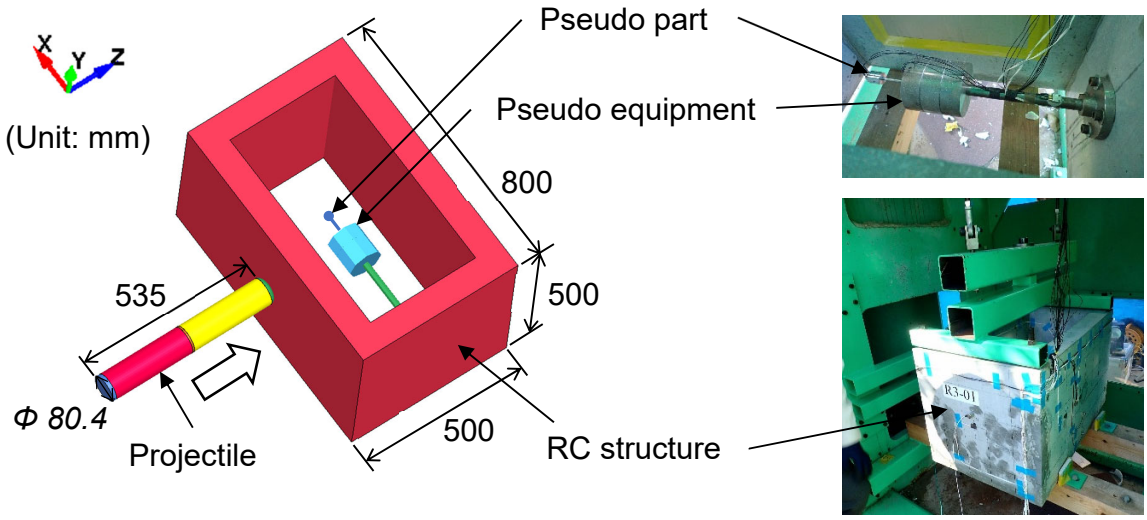

Figure 2. Outline of the projectile impact test.

Table 1: Specifications of the RC structure.

Average Compressive strength	40.8 N/mm^2 (28days) 45.0 N/mm^2 (47days)
Rebar diameter	6mm
Rebar layers	2 layers
Reinforcement ratio	1.1 %
Covering thickness	10 mm

Projectile

The shape of the projectile simulating an aircraft was a thin-walled cylindrical two-chamber structure, based on Borschnek et al. (2013), with the aim of approximately 1/70 of the actual aircraft size. Figure 3 shows the projectile schematics. The thickness of the tip (semi-elliptical spherical shell structure) and the first chamber was 0.3 mm, and the second chamber was 0.5 mm thick (Fig.3). A partition plate was installed at the boundary between the first and second chambers and the tail end.

The cylinders of the two chambers were welded with longitudinal seams using carbon steel (SPCC as the Japanese Industrial Standard (JIS) G3141), and the joint between the tip and the cylinders was circumferentially welded. The partition plate was also carbon steel (SS400 as JIS G3101) welded to the cylindrical part. Table s shows the mill sheets of the SPCC and SS400 materials used for the projectile.

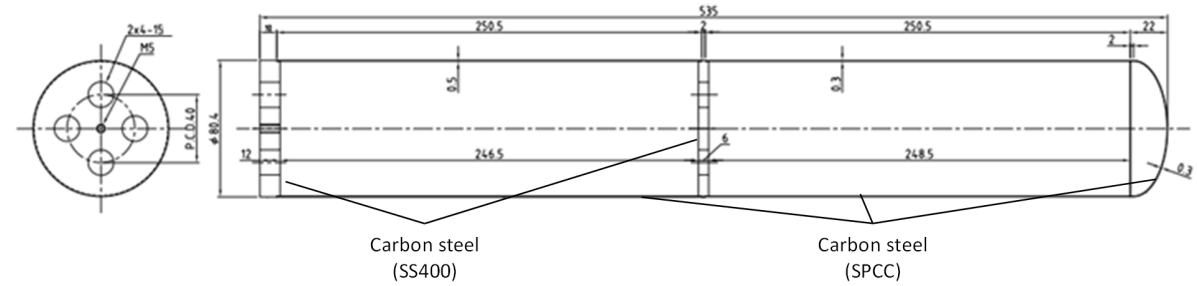

Figure 3. Projectile schematics (unit: mm).

Table 2: The structural specifications of the projectile.

Item	Yield stress (N/mm^2)	Ultimate stress (N/mm^2)	Elongation (%)
SPCC (JIS G3141)	225	348	40
SS400 (JIS G3101)	314	467	31

Measuring method

The measurement parameters included impact velocity, acceleration, strain, and high-speed photography. The impact velocity was calculated using the transit time for a predetermined 200 mm section of the launch device (Fig. 1).

Acceleration was measured at six locations and in triaxial directions on the RC structure and pseudo equipment. Figure 4 shows the accelerometer locations. Accelerometers were employed with 50,000 m/s^2 capacity for the high acceleration generated on the RC structure due to the projectile impact. Figure 4 also shows the strain gage locations. An enamel floor was placed on the concrete surface of the RC structure and strain gauges were attached with their axes aligned in the propagation direction from the impact surface.

The impact behavior on the impact face was captured using a high-speed camera placed on the front side (impact side) of the RC structure. During the impact test, shooting speed of the camera was 10,000 frames per second.

TEST RESULTS

Static compression test of the projectile

To understand the static buckling behavior as a reference for projectile deformation in the impact tests, a static compression test of the projectile was conducted using a 1,000 kN press testing machine. The projectile was installed vertically in the axial direction, with the head pointing upward and the tail on the bed surface plate side.

Figure 5 shows the force-displacement relationship for the static compression test. A standard head speed of 6 mm/min (0.1 mm/s) was selected, and the test was conducted at a test quasi-static speed. Consequently, square-tube deformation developed in the center of the thin-walled cylindrical section, and buckling progressed as the wrinkles folded. Finally, all thin-walled cylindrical sections buckled, and stable yield buckling forces and subsequent plateau forces could be measured in the first and second chambers.

The two peak loads are the buckling loads when the first and second chambers begin to buckle, and the second peak is larger than the first peak because the second chamber is thicker than the first.

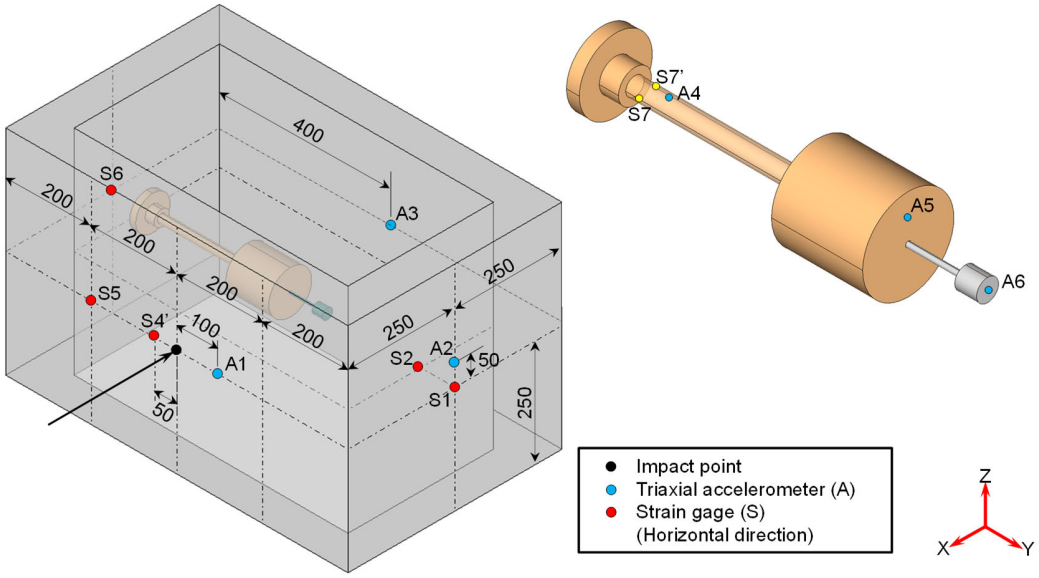

Figure 4. The location of accelerators and strain gages.

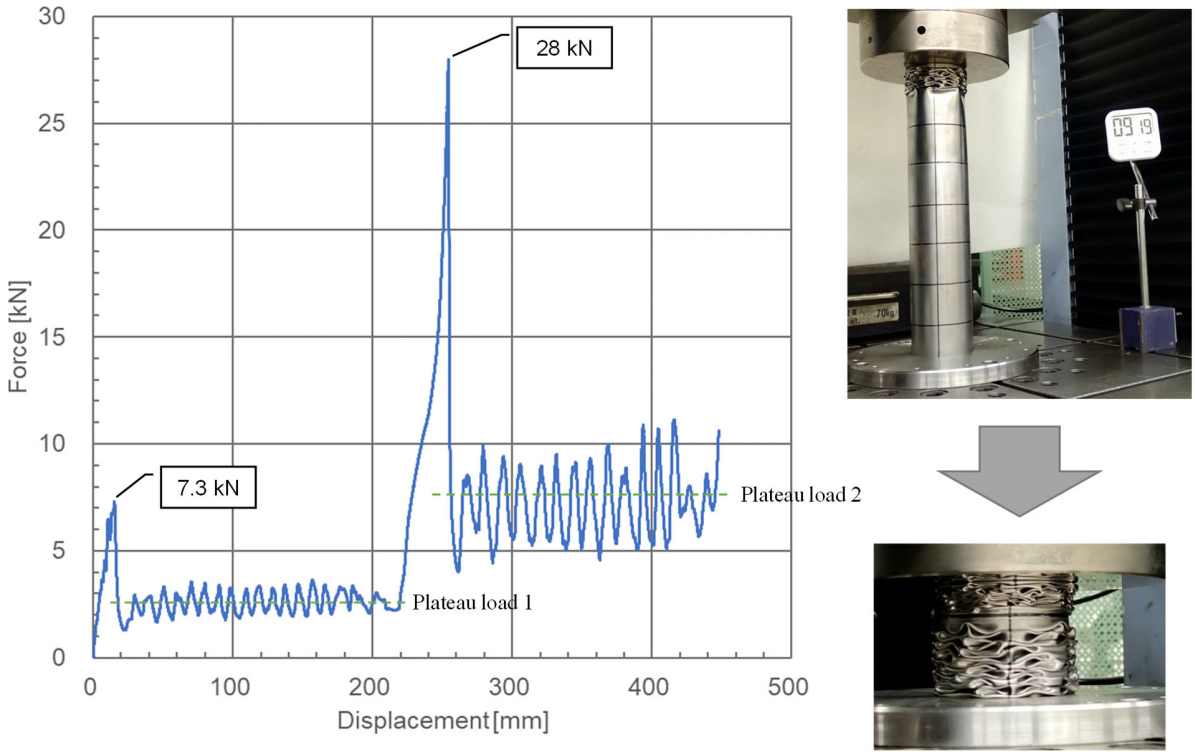

Figure 5. Force-displacement relationship for the static compression test.

Impact force measurement test

The maximum impact force was investigated by measuring the impact forces at the impact velocities used in the impact test before the projectile impact test. Impact force measurement tests were conducted in two cases of lower impact velocity (61 m/s) and higher velocity (132 m/s).

The maximum impact forces were measured using a load cell, and Fig. 6 shows the results. The second reaction force, caused by the impact of the partition plate, was measured at approximately 1.5 ms.

Table3 summarizes the test conditions and the maximum impact forces for the test. The impact velocity ratio was approximately equal to the maximum impact force ratio and showed a reasonable trend because stress and velocity are proportional in stress wave propagation in elastic bodies (Timoshenko and Goodier (1970)).

Table 3: Test conditions of the impact force measurement tests.

Case	Impact velocity (m/s)	Maximum impact force (kN)
R3-101	61	150
R3-102	132	360
Ratio	2.2	2.4

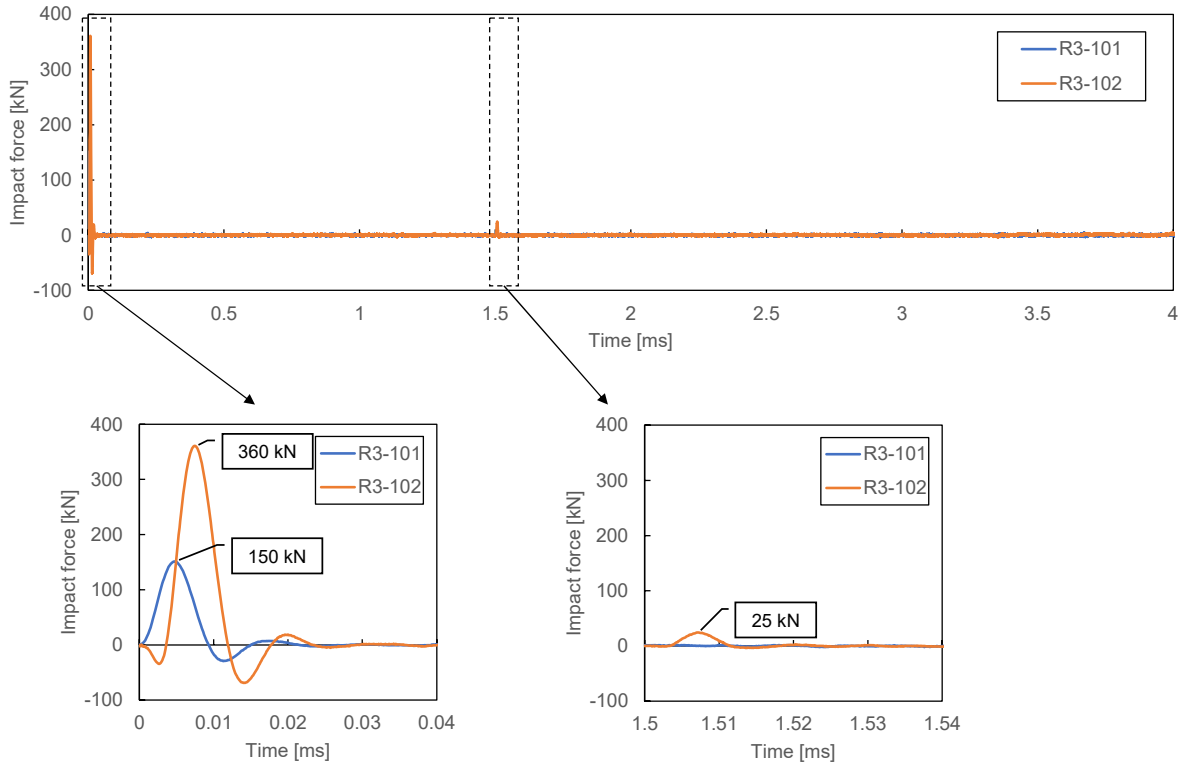

Figure 6. Time history of the reaction force for the impact force measurement test.

Projectile impact test

Projectile impact tests investigated the impact response by varying the projectile velocities; therefore, lower impact velocities of approximately 60 m/s and higher impact velocities above 150 m/s were adopted. Table 4 summarizes the test results in these three cases. In the third case, cracking on the rear surface of the impact wall was found in the RC structure.

Figure 7 shows still images from high-speed shooting on the impact surface in Case R3-03. The first and second chambers of the projectile gradually buckled, and the projectile was almost crushed after the test.

Table 4: Summary of the test results.

Case	Impact velocity (m/s)	Damage
R3-01	62	No
R3-02	157	No
R3-03	172	Cracks on the rear surface

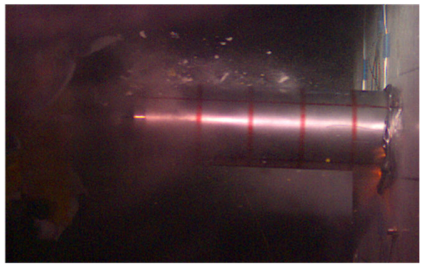

(a) Around 2.3 ms after impact

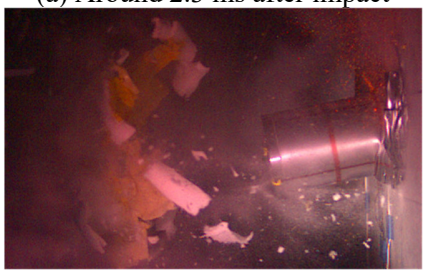

(b) Around 2.9 ms after impact

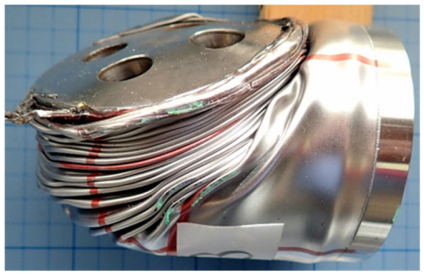

(c) After the impact test

Figure 7. Still images from high-speed shooting on the impact surface (Case R3-03)

The accelerations were measured on the RC structure and pseudo equipment. Figure 8 shows the acceleration time history in the x-direction in Case R3-03 separately for the RC structure and pseudo equipment. The acceleration of A1 attached to the impact surface indicates a steep and high acceleration associated with the impact (excluded from this figure). Figure 8(a) shows sharp history of the RC structure, while Figure 8(b) shows stable vibration of the pseudo equipment. The acceleration of A4X presents high-peak input acceleration, whereas the accelerations of A5X and A6X present stable vibration. In other words, for high-input acceleration, response reduction was observed in the pseudo equipment, responding according to the primary dominant frequency. Furthermore, Figure 9 shows the estimated displacement evaluated by integrating the acceleration separately for the RC structure and pseudo equipment. The estimated displacement presents stable vibration on the pseudo equipment and part.

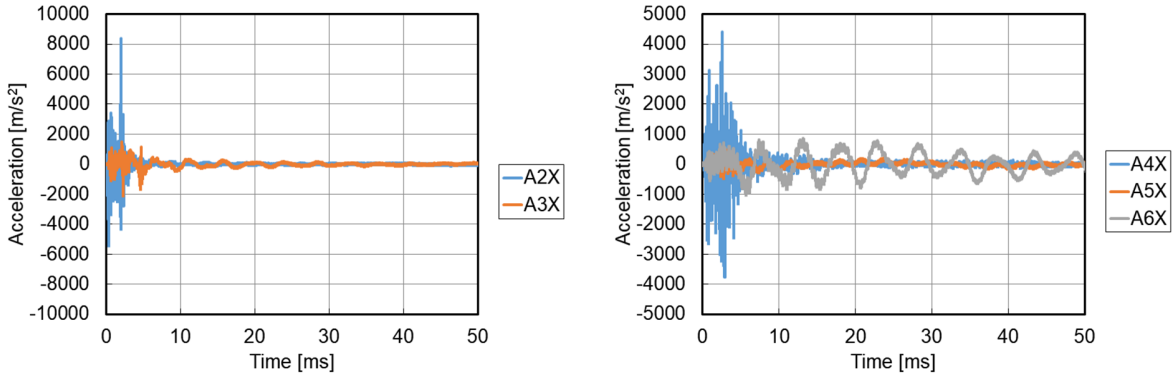

(a) RC structure (A2–A3) (b) Pseudo equipment (A4–A6)

Figure 8. Time histories of the impact test accelerations of Case R3-03.

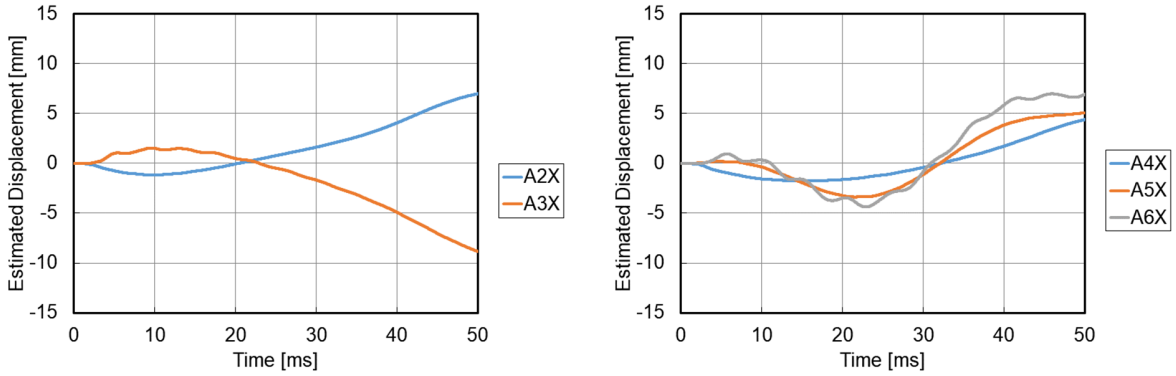

(a) RC structure (A2–A3) (b) Pseudo equipment (A4–A6)

Figure 9. Estimated displacement for the impact test of Case R3-03.

Figure 10 shows the Fourier spectrum of the accelerations on the pseudo equipment. The Fourier spectrum shows a primary dominant frequency of approximately 38 Hz, a secondary dominant frequency of approximately 340 Hz for the pseudo equipment and a primary dominant frequency of approximately 200 Hz for the pseudo part. The acceleration of the pseudo part provides a mixed dominant frequency response, including the dominant frequencies of the pseudo equipment and the pseudo part.

Figure 11 shows response strains at the pseudo equipment. The strain time histories of S7 and S7′ are equal in magnitude and opposite in positive and negative, indicating that the bending vibration mode is the dominant response of the pseudo equipment. The dominant frequency of the pseudo equipment can be approximately 38 Hz from the period of vibration, corresponding with the primary dominant frequency of the pseudo equipment.

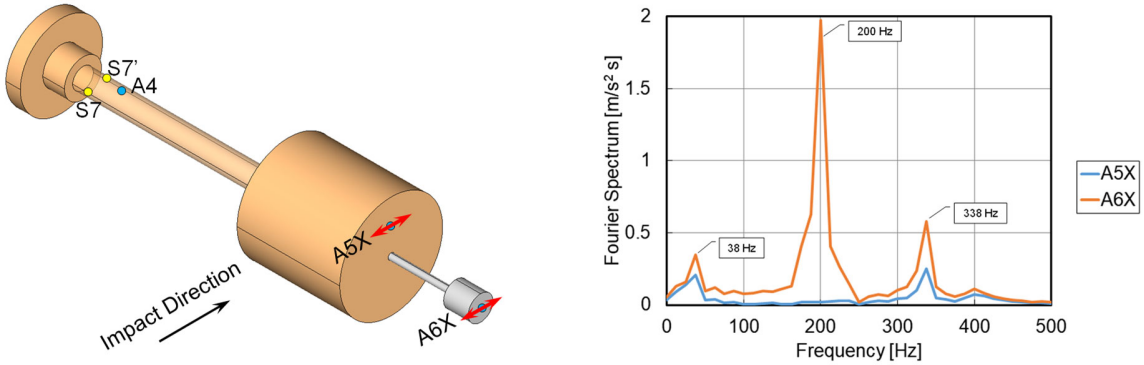

Figure 10. Fourier spectra of the accelerations attached on the pseudo equipment.

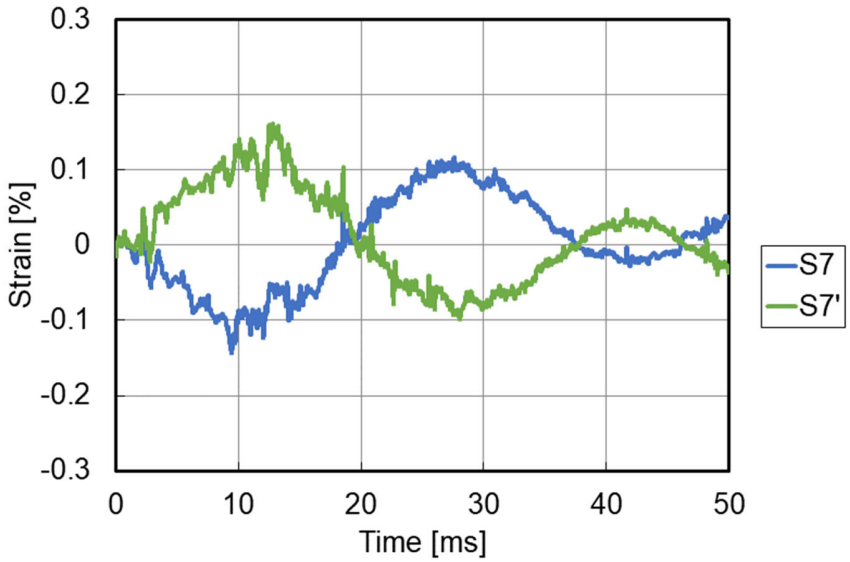

Figure 11. Response strains at the pseudo equipment.

SUMMARY AND CONCLUSIONS

This study conducted a series of projectile impact tests on an RC structure that models a nuclear building with internal equipment and its part. In the third case, cracking on the rear surface of the impact wall was found in the RC structure. After the tests, the impact response characteristics of the RC structure, pseudo equipment and pseudo part were investigated and the following was observed from the test results.

- For the static compression test of the projectile, a square-tube deformation developed in the center of the thin-walled cylindrical section, and buckling progressed as the wrinkles folded. Finally, all thin-walled cylindrical sections buckled, and stable yield buckling forces and subsequent plateau forces could be measured in the first and second chambers.
- The impact force measurement test measured the impact forces using load cells. The impact velocity ratio was approximately equal to the maximum impact force ratio, showing a reasonable trend because stress and velocity are proportional in stress wave propagation in elastic bodies.
- The following results were obtained from the impact tests.
  - Response reduction was observed in the pseudo equipment for high-input acceleration, responding according to the primary dominant frequency.
  - The acceleration of the pseudo part provided a mixed dominant frequency response, including dominant frequencies of the pseudo equipment and the pseudo part.
  - The dominant frequency of the pseudo equipment can be approximately 38 Hz from the period of vibration, corresponding to the primary dominant frequency of the pseudo equipment.

We intend to perform a detailed analysis of the test results for future studies, focusing on the impact response behavior of the pseudo equipment.

REFERENCES

Borschnek, F., Herrmann, N., Müller, H. S. (2013). “Numerical Simulation of the Impact of Fluid-Filled Projectiles Using Realistic Material Models”; Trans. SMiRT-22, San Francisco, CA, USA.

Kennedy, R.P., (1976). “A review of procedure for the analysis and design of concrete structures to resist missile impact effects”, Nucl. Eng. Des. 37, 183-203.

Li, Q.M., Reid, S., Wen, H. M., Telford A. R., (2005). “Local impact effects of hard missiles on concrete targets”, Int. J. Impact Eng. 32, 224-284.

NEA/CSNI/IRIS_2010 R(2011)8, 2011. Improving Robustness Assessment Methodologies for Structures Impacted by Missiles (IRIS_2010) Final Report. Published by OECD.

Timoshenko, S. P., Goodier, J. N. (1970). "Theory of Elasticity", McGraw-Hill.